Transgenic Mouse Proteomics Identifies New 14-3-3-associated Proteins Involved in Cytoskeletal Rearrangements and Cell Signaling*[S]

Pierre-Olivier Angrand‡§¶, Inmaculada Segura‖, Pamela Völkel‡§, Sonja Ghidelli‡, Rebecca Terry‖, Miro Brajenovic‡, Kristina Vintersten‡‡§§, Rüdiger Klein‖, Giulio Superti-Furga‡¶¶, Gerard Drewes‡, Bernhard Kuster‡, Tewis Bouwmeester‡, and Amparo Acker-Palmer‖ ||||**

Identification of protein-protein interactions is crucial for unraveling cellular processes and biochemical mechanisms of signal transduction. Here we describe, for the first time, the application of the tandem affinity purification (TAP) and LC-MS method to the characterization of protein complexes from transgenic mice. The TAP strategy developed in transgenic mice allows the emplacement of complexes in their physiological environment in contact with proteins that might only be specifically expressed in certain tissues while simultaneously ensuring the right stoichiometry of the TAP protein *versus* their binding partners and represents a novelty in proteomics approaches used so far. Mouse lines expressing TAP-tagged 14-3-3ζ protein were generated, and protein interactions were determined. 14-3-3 proteins are general regulators of cell signaling and represent up to 1% of the total brain protein. This study allowed the identification of almost 40 novel 14-3-3ζ-binding proteins. Biochemical and functional characterization of some of these interactions revealed new mechanisms of action of 14-3-3ζ in several signaling pathways, such as glutamate receptor signaling via binding to homer homolog 3 (Homer 3) and in cytoskeletal rearrangements and spine morphogenesis by binding and regulating the activity of the signaling complex formed by G protein-coupled receptor kinase-interactor 1 (GIT1) and p21-activated kinase-interacting exchange factor β (βPIX). ***Molecular & Cellular Proteomics 5: 2211–2227, 2006.***

Most cellular processes are carried out by a multitude of proteins that assemble into multimeric complexes. A precise understanding of the biological pathways that control cellular processes relies on the identification and biochemical characterization of the proteins involved in such multimeric complexes.

14-3-3 proteins are highly conserved small acidic proteins encoded by seven mammalian genes (α/β, ε, η, γ, τ/θ, ζ/δ, and σ). These proteins have been implicated in the regulation of a wide variety of both general and specialized signaling pathways (for a review, see Ref. 1). In most cases, 14-3-3 proteins regulate cellular processes by binding to specific Ser(P) and Thr(P) motifs within target proteins (2). Two optimal 14-3-3 phosphopeptide ligands with the consensus sequences RS*X*(pS/T)*X*P and R*X*(Y/F)*X*(pS/T)*X*P (where pS/T represents phosphoserine or phosphothreonine and *X* is any amino acid) have been defined (3). However, some 14-3-3 proteins bind to phosphorylated motifs that differ from the consensus or even bind to unphosphorylated motifs (4). For all their regulatory functions 14-3-3 proteins need to associate in stable homo- and heterodimers (5). The complexity of 14-3-3 actions is reflected by the increasing number of binding partners that have been identified. Several studies have used tagged 14-3-3 proteins to purify protein complexes from cells in culture (6–9). 14-3-3 proteins are abundant in brain tissues, and although only a few binding partners in brain have been postulated so far, 14-3-3 proteins are clearly critical for brain development, memory, and learning and have been implicated as well in several neurological disorders (for a review, see Ref. 1).

To identify new roles of 14-3-3 proteins, we used a directed proteomics analysis of 14-3-3ζ-binding proteins in the brain of transgenic mice using the tandem affinity purification (TAP)[1]-MS methodology. TAP was developed as a generic

From the ‡Cellzome AG and the ‡‡European Molecular Biology Laboratory, Meyerhofstrasse 1, D-69117 Heidelberg, Germany and ‖Max Planck Institute of Neurobiology, Am Klopferspitz 18, D-82152 Martinsried, Germany

Received, April 19, 2006, and in revised form, July 18, 2006

Published, MCP Papers in Press, September 6, 2006, DOI 10.1074/mcp.M600147-MCP200

[1] The abbreviations used are: TAP, tandem affinity purification; Homer 3, homer homolog 3; GIT, G protein-coupled receptor kinase interactor; PIX, PAK-interacting exchange factor; TEV, tobacco etch virus; Cdc, cell division cycle; AK, adenylate kinase; PAK, p21-activated kinase; LDB, LIM domain binding; PDE, phosphodiesterase; MADD, mitogen-activated protein kinase-activating death domain; SMARCB, SWI/SNF-related matrix-associated actin-dependent reg-

method to efficiently purify protein complexes from cells in culture (for a review, see Ref. 10). Two affinity tags, protein A and calmodulin-binding peptide separated by a tobacco etch virus (TEV) protease cleavage site are fused to the protein of interest. In addition to numerous applications in bacteria, yeast, worms, and flies, this approach was previously used in human cells in culture to map the tumor necrosis factor α/nuclear factor-κ-B pathway (11) and to map a protein interaction network between the partitioning-defective (PAR) proteins involved in mammalian cell polarity (9). Here we demonstrate that the TAP-MS method can also be applied to transgenic mice to characterize *in vivo* protein-protein interactions in mouse tissues. In this study, mouse lines expressing tagged 14-3-3ζ were generated, and protein interactions were determined. This approach led to the identification of new, tissue-specific 14-3-3ζ binding partners not previously identified from the cultured cell models. Moreover we describe new mechanisms of action of 14-3-3 proteins in several signaling pathways, such as in the glutamate receptor signaling via binding to Homer 3 and in cytoskeletal rearrangements in migrating cells and spine morphogenesis in neurons by binding to the signaling complex formed by GIT1 and PIX.

EXPERIMENTAL PROCEDURES

cDNA Cloning and Transgenic Vector Engineering—Expression vectors were generated by site-specific recombination (Gateway system, Invitrogen) of PCR-amplified ORFs into TAP-, hemagglutinin (HA) epitope-, myelocytomatosis (Myc) oncogene epitope-, yellow fluorescent protein (YFP)-, or cyan fluorescent protein (CFP)-tagged versions of the Moloney murine leukemia virus-based vector pZome1 (Cellzome; available from Euroscarf GmbH). All the ORFs were tagged at the 5′-end. The inserted ORFs were subcloned from the following human Mammalian Gene Collection cDNA clones: 14-3-3ζ, IMAGE: 2988020; adenylate kinase isoenzyme 5 (AK5), IMAGE:4816351; LIM domain binding (LDB) 1, IMAGE:2964724; phosphodiesterase (PDE) 1A, IMAGE:4814064; and mitogen-activated protein kinase-activating death domain (MADD), IMAGE:5271798. cDNAs for βPIX and GIT1 were kindly provided by Dr. Richard Premont (Duke University Medical Center). The double mutant R56A/R60A (14-3-3-DN) of 14-3-3ζ was generated by PCR-based site-specific mutagenesis on YFP-tagged 14-3-3ζ construct using the primers described before (12). The pUbi-CTAPgw expression vector was constructed by PCR subcloning the human UbiC promoter from position −1225 to −6 and the SV40 poly(A) signal from pUbi-cJun (13) into pBluescript KS (Stratagene, La Jolla, CA). Subsequently a TAP cassette from pZome1 and the Gateway recombination cassette (Invitrogen) were inserted between the promoter and the polyadenylation signal. Unique restriction sites flanking the expression unit allows the removal of the prokaryotic vector sequences prior to oocyte injection. Transgenic vectors were generated by site-specific recombination (Gateway system, Invitrogen) of PCR-amplified ORFs to obtain pUbi-NTAP-14-3-3ζ.

Production of TAP Transgenic Mice—All animal experiments were conducted in a licensed animal facility in accordance with German Animal Welfare Act (Tierschutzgesetz) following the guidelines of the European Convention for Protection of Vertebrate Animals Used for Experimental and Other Scientific Purposes (1986). The production of transgenic mice was carried out essentially as described before (14). The plasmid pUbi-NTAP-14-3-3ζ was digested with NsiI and KpnI, and the 3.9-kbp fragment, corresponding to the expression cassette, was gel-purified with the Qiagen gel purification kit according to the manufacturer's protocol (Qiagen, Hilden, Germany) and diluted to 1.5 ng/μl in injection buffer. Fertilized oocytes were collected from superovulated C57BL/6J female mice and mated with C57BL/6J males. The purified Ubi-NTAP-14-3-3ζ transgene was microinjected into the pronuclei, and the embryo was transferred to the oviduct of 0.5-day postcoitus pseudopregnant outbred recipients 5–6 h following injection. Progeny were genotyped by PCR analysis using the oligomers 5′-CACCCGTTCTGTTGGCTTAT-3′ (specific to human UbiC promoter sequences) and 5′-TGGCTGCTGAGACGGCTATGA-3′ (specific to the TAP cassette). Founders were mated onto CD1 outbred background to produce hemizygous animals for further characterization and TAP-MS studies.

Tandem Affinity Purification—The material corresponding to 15 perfused transgenic brains, five perfused transgenic livers, or 15 perfused transgenic hearts were homogenized in a Dounce homogenizer in 10 ml of lysis buffer (250 mM Tris-HCl, pH 7.5, 25% glycerol, 7.5 mM $MgCl_2$, 0.5% (v/v) Triton X-100, 500 mM NaCl, 125 mM NaF, 5 mM Na_3VO_4, 1 mM DTT, 1% Complete (Roche Applied Science)), and two independent TAPs were performed. Two affinity tags, protein A and calmodulin-binding peptide, separated by a TEV protease cleavage site constitute the TAP tag (15). The first purification step involves the binding of protein A to IgG beads. The elution of the bound material is achieved by incubation with the TEV protease. This elution strategy significantly reduces background due to nonspecific binding to the column. The eluate is then further purified on calmodulin-coated beads to remove the TEV protease as well as additional contaminants. Purified protein complexes are finally eluted with calcium chelating agents. For the purification, lysates were cleared by centrifugation and incubated with 200 μl of IgG-agarose beads (Sigma) for 2 h at 4 °C. The beads were collected in 0.8-ml spin columns (MoBiTec, Goettingen, Germany) and washed with cleavage buffer (10 mM Tris-HCl, pH 7.5, 100 mM NaCl, 1 mM DTT, 0.1% Nonidet P-40, 0.5 mM EDTA). The beads were resuspended in cleavage buffer and incubated with 100 units of TEV protease (Invitrogen) for 1 h at 16 °C. The eluate was transferred into a column containing 200 μl of calmodulin-agarose (Stratagene) in 10 mM Tris-HCl, pH 7.5, 100 mM NaCl, 1 mM DTT, 0.1% Nonidet P-40, 2 mM $MgCl_2$, 2 mM imidazole, 4 mM $CaCl_2$, and after washing with excess buffer, the column was eluted with 600 μl of elution buffer (10 mM Tris-HCl, pH 8.0, 5 mM EGTA) at 37 °C. The freeze dried eluates were separated on 4–12% NuPAGE Novex gels (Invitrogen) and stained with colloidal Coomassie.

Protein Digestion and Mass Spectrometry—Gels were sliced into 24 bands across the entire separation range of each lane. Cut bands were reduced, alkylated with iodoacetamide, and in-gel digested with trypsin (Promega) as described previously (16). Each tryptic digest sample was subjected to LC-MS/MS analysis as follows. Peptides were separated on a self-packed 75-μm-inner diameter × 15-cm column (ReproSil-Pur 120 C_{18}-AQ 5 μm, Dr. Maisch, Ammerbuch, Germany) at a flow rate of ~250 nl/min delivered by a CapLC nano-LC system (Waters, Eschborn, Germany) and the following solvent scheme: solvent A, 0.1% formic acid; solvent B, 70% acetonitrile in 0.1% formic acid. Samples were loaded in solvent A, and peptides were eluted by 10% solvent B for 5 min followed by a linear gradient

ulator of chromatin subfamily B; CFP, cyan fluorescent protein; MARK, microtubule-associated protein/mi crotubule affinity-regulating kinases; AMPA, α-amino-3-hydroxy-5-methyl-4-isoxazole propionate; GEF, guanine nucleotide exchange factor; YFP, yellow fluorescent protein; GRIP, glutamate receptor-interacting protein; HEK, human embryonic kidney; PAP, peroxidase-anti-peroxidase; HDAC, histone deacetylase; mGluR, metabotropic glutamate receptor; DN, dominant negative; E, embryonic day; DIV, days *in vitro*.

to 60% solvent B in 40 min and holding the column at 90% solvent B for 5 min before re-equilibrating the system for 10 min using 10% solvent B. Up to three peptide precursor ions were subjected to data-dependent acquisition of tandem mass spectra using a Q-Tof II mass spectrometer (Waters).

Protein Identification—Tandem mass spectra were converted into peak lists using MassLynx (version 3.4, Waters) and subjected to automated database searching (Mascot version 1.8, Matrix Science) against an in-house curated version of the International Protein Index comprising >200,000 human and mouse protein sequences (IPI, human versions 2.5–2.18, mouse versions 1.0–1.10, European Bioinformatics Institute, www.ebi.ac.uk/IPI/). This set of sequences was complemented with frequently observed laboratory contaminants (such as sheep keratins), viral proteins expressed by the examined immortalized cell lines, and sequences of epitope-tagged proteins under investigation. Search parameters were: MS and MS/MS tolerance, 0.4 Da; tryptic specificity allowing for up to three missed cleavages and (K/R) ↓ P cleavages (to account for in-source fragmentation); fixed modification, carbamidomethylation of cysteine; variable modification, oxidation of methionine. Search results were read into a proprietary Oracle database for further data analysis. Most proteins were unambiguously identified by the sequencing of several independent peptides. We categorically rejected identifications with Mascot scores indicating a higher than 5% probability that the match could be a random event (17). In addition, for single peptide identifications, we required the reported peptide to have an at least 10-fold higher probability to be a non-random event than the next best peptide candidate suggested by Mascot. All identified proteins and peptides are provided in Supplemental Tables S1 and S2.

Cell Culture—Human adenocarcinoma HeLa cells and human embryonic kidney (HEK) 293 cells were cultured in Dulbecco's modified Eagle's medium (Invitrogen) supplemented with 10% fetal bovine serum (Invitrogen), 2 mM L-glutamine, and penicillin/streptomycin (both from PAA Laboratories GmbH, Linz, Austria). The SK-N-BE(2) neuroblastoma cell line was cultured in Opti-MEM-GlutaMAX (Invitrogen) supplemented with 10% iron-enriched fetal bovine serum (Sigma) and penicillin/streptomycin. For biochemical analysis of the interactions, HeLa cells were transiently transfected with HA-14-3-3ζ together with every interactor tagged to CFP using Effectene transfection reagent (Qiagen). HEK293 cells were transiently transfected with Myc-14-3-3ζ, -β, -η, or -γ together with MARK2, MARK3, or MARK4 tagged with HA. For immunofluorescence analysis, HeLa cells were transfected with YFP-14-3-3ζ together with βPIX-FLAG, and SK-N-BE(2) cells were single transfected with CFP-Homer 3. All transfections for immunofluorescence were done with the calcium phosphate-DNA precipitation method.

For cell fractionation, cells were scraped in chilled non-detergent LBB lysis buffer (50 mM Tris-HCl (pH 7.5), 150 mM NaCl, 10 mM $NaPP_i$, 20 mM NaF, 1 mM sodium orthovanadate, 1× Complete), homogenized in a Dounce homogenizer 30 times at 4 °C, and centrifuged (600 × *g*, 10 min, 4 °C). Supernatants containing cytoplasmic proteins were stored, and the pellets, containing the unbroken nuclei, were incubated in LBA buffer (50 mM Tris-HCl (pH 7.5), 0.5% Nonidet P-40, 150 mM NaCl, 10% glycerol, 10 mM $NaPP_i$, 20 mM NaF, 1 mM sodium orthovanadate, 1× Complete) for 10 min at 4 °C. Supernatants containing the nuclear proteins were collected after centrifugation (16,000 × *g*, 10 min, 4 °C).

For α-amino-3-hydroxy-5-methyl-4-isoxazole propionate (AMPA) stimulation, transfected SK-N-BE(2) cells were starved for 24 h as above and stimulated for 10 min with 100 μM (*S*)-AMPA (Tocris, Bristol, UK). For hippocampal neuron cultures, hippocampi from embryonic day 18 Sprague-Dawley rats were separated from diencephalic structures and digested with 0.25% trypsin (Invitrogen) for 20 min at 37 °C with gentle shaking. Cells were plated and grown in Neurobasal medium supplemented with B27 (Invitrogen). Neurons were plated on coverslips coated with poly-D-lysine (1 mg/ml) and laminin (5 μg/ml) at a density of 50,000/well and transfected by a calcium phosphate-DNA precipitation procedure.

Rac and Cdc42 Activated Pulldown Assays—Transfected HeLa cells were starved for 48 h, washed two times with chilled TBS buffer, and lysed in RPL buffer (50 mM Tris-HCl (pH 7.5), 1% Nonidet P-40, 200 mM NaCl, 5 mM $MgCl_2$, 1 mM DTT, 10% glycerol, 20 mM NaF, 1 mM sodium orthovanadate, 1× Complete EDTA-free). 25 μg of recombinant bacterially produced GST-PAK were prebound to 20 μl of glutathione-Sepharose beads (Amersham Biosciences) and then incubated for 1 h at 4 °C with 500 μg of protein lysates. After incubation, beads were washed three times with RPL buffer. Samples were analyzed by SDS-PAGE and Western blotting with anti-Rac or anti-Cdc42 antibodies (BD Biosciences).

Immunoblotting and Immunoprecipitation—For immunoprecipitation, 20 μl of protein A-Sepharose beads (Amersham Biosciences) were washed with PBS and incubated with 10 μl of anti-HA (12CA5; Roche Applied Science) or 4 μl of anti-Myc (9E10; Santa Cruz Biotechnologies, Santa Cruz, CA) antibodies for 1 h at room temperature. Equivalent protein levels from the lysates were incubated with these beads at 4 °C. After 2 h of incubation, samples were washed three times with LBA buffer and separated by SDS-PAGE. For immunoblotting, protein samples were separated by 6, 8, or 12% SDS-PAGE and transferred to 0.2-μm nitrocellulose membranes (Schleicher & Schuell). Membranes were incubated with antibodies anti-HA, anti-Myc, anti-FLAG (M2; Sigma), anti-green fluorescent protein (JL-8; BD Biosciences), or anti-14-3-3 (H-8; Santa Cruz Biotechnologies). TAP proteins were detected using peroxidase-anti-peroxidase (PAP) antibody (Sigma). Secondary antibody goat anti-mouse conjugated with horseradish peroxidase (Jackson Immunoresearch, West Grove, PA) and ECL reagent (Amersham Biosciences) were used.

Cerebella or whole brains were excised from 8-week-old CD1 mice. Samples were washed in cold PBS and homogenized in a Dounce homogenizer 30 times in LBA buffer. Homogenates were centrifuged (16,000 × *g*, 10 min, 4 °C), and supernatants (4 mg of protein) were incubated either with protein A-Sepharose beads (Amersham Biosciences) prebound to rabbit preimmune serum, anti-GIT1, anti-αPIX, or anti-βPIX antibodies (kindly provided by Dr. Richard Premont); with protein G-Sepharose beads (Amersham Biosciences) prebound to rat preimmune serum or anti-Homer antibody (Chemicon, Temecula, CA); or with anti-14-3-3-agarose-conjugated beads (K-19; Santa Cruz Biotechnologies). Western blots were incubated with the corresponding antibodies mentioned above, with anti-14-3-3 (H-8; Santa Cruz Biotechnologies), or with anti-phospho(Ser)-14-3-3 binding motif antibody (9601; Cell Signaling Technology).

Immunofluorescence—Cells were seeded on untreated or laminin-coated coverslips. After starving and/or stimulation, cells were fixed with 4% paraformaldehyde for 15 min at 4 °C and rinsed once with PBS. To detect transfected or endogenous non-fluorescent proteins, cells were permeabilized with PBS, 0.5% Triton X-100 (PBS-T) for 15 min and blocked for 60 min with PBS-T, 5% goat, 5% donkey sera (Jackson Immunoresearch). Samples were incubated with primary rabbit anti-14-3-3 (Upstate Biotechnology, Lake Placid, NY) antibody for 1 h. After three washes in PBS-T, samples were incubated with Cy3-conjugated goat anti-rabbit (Jackson Immunoresearch). Incubations were made at room temperature. Neurons were stained with Cy3-conjugated anti-Myc antibody (Sigma). When indicated actin was stained with Texas Red-conjugated phalloidin (Jackson Immunoresearch). After washing, samples were mounted using the ProLong antifade kit (Molecular Probes, Eugene, OR). Images were ac-

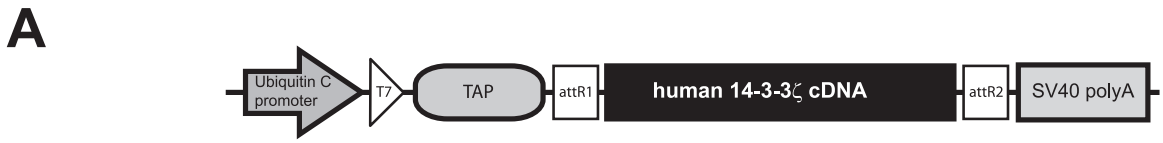

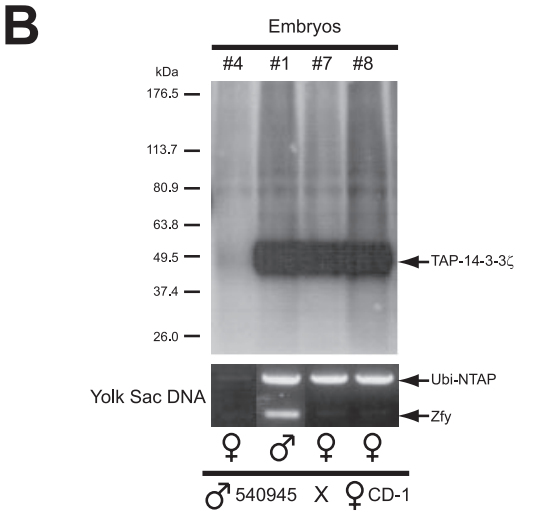

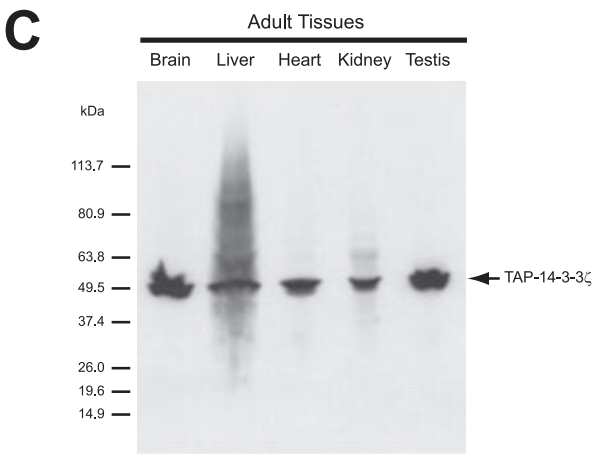

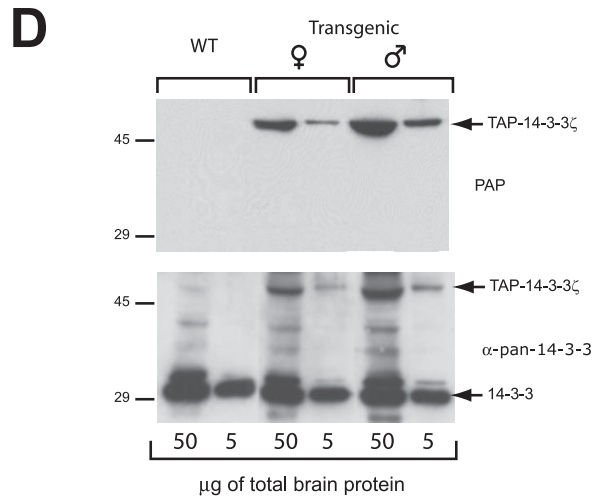

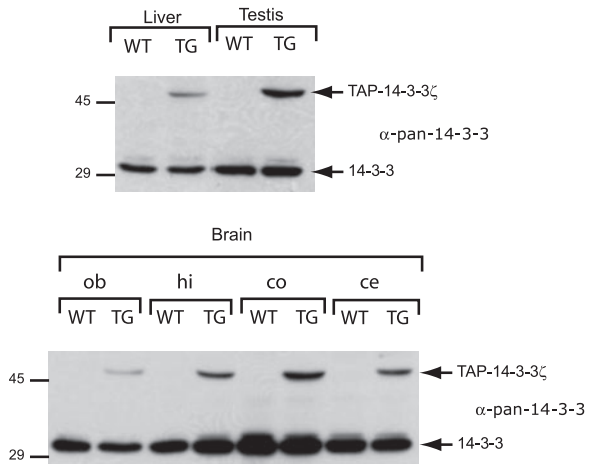

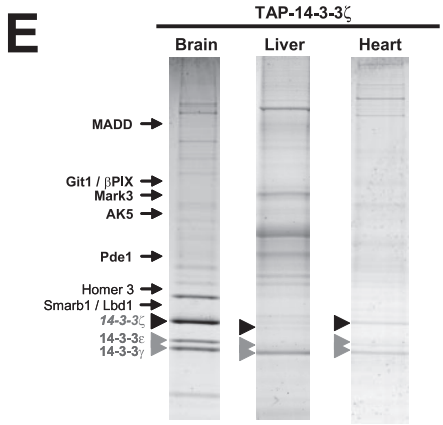

quired using an epifluorescence microscope (Zeiss, Goettingen, Germany) equipped with a digital camera (SpotRT; Diagnostic Instruments, Sterling Heights, MI) and analyzed with MetaMorph software (Visitron, Munich, Germany).

RESULTS

Isolation of 14-3-3 Protein Complexes from Transgenic Mice

Transgenic mouse lines expressing TAP-tagged 14-3-3ζ were generated by oocyte injection. For this study, we generated vectors containing the human ubiquitin C promoter driving ubiquitous expression of chimeric TAP-14-3-3ζ with the TAP tag at the N terminus of the protein (Fig. 1*A*). A total of eight transgenic founder mice (two males and six females) were identified by PCR-based genotyping. All of them were fertile as judged by their ability to produce offspring over a 6-month period. Expression of TAP-14-3-3ζ was not associated to notable developmental or behavioral phenotypes when compared with wild-type lines. Although the protein A moiety of the TAP tag might interact with mouse circulating IgGs, no side effects such as toxicity or autoimmune reactions were observed in the transgenic lines expressing TAP-tagged 14-3-3ζ. The line 540945 derived from a male founder was used for further characterization and TAPs. As expected, TAP-14-3-3ζ transgene expression was detected in all tissues examined as well as in embryos (Fig. 1, *B* and *C*). Importantly the expression level of TAP-14-3-3ζ is in the same range as the endogenous brain expression of 14-3-3 proteins avoiding problems typically associated with overexpression that can lead to non-physiological interactions (Fig. 1*D*).

Prior to organ extractions, transgenic mice were perfused with PBS to avoid interaction of the protein A moiety of the TAP cassette with circulating mouse IgGs. After organ extraction, protein extracts were subjected to TAP. Isolated protein complexes were analyzed by LC-MS/MS and assigned to specific proteins with the Mascot search engine. As expected, the most prominent TAP-14-3-3ζ binding partners identified from brain, liver, and heart were the other endogenous 14-3-3 isotypes (Fig. 1*E*), indicating that the TAP method could be applied to transgenic mice in a direct *in vivo* proteomics study.

Transgenic Mouse Proteomics Allows the Identification of Novel 14-3-3 Binding Partners

Because a number of proteins are expressed in a tissue-restricted fashion, purification of protein complexes from mouse tissues is expected to give new insights on the tissue-specific binding partners of a given protein. From two independent TAP experiments from transgenic mouse brains, we identified a total of 147 proteins (Supplemental Table S1). All protein identification data are available in Supplemental Tables S1 and S2. Table I presents about 60 14-3-3ζ-associated proteins, which include 11 signaling kinases, 11 phosphatases and phosphodiesterases, 12 small GTPase-related proteins, six cytoskeleton related proteins, six signaling adaptor proteins, metabolic enzymes, proteins involved in cellular and vesicle trafficking, ion channels, transcription factors, and proteins that participate in the regulation of chromatin structure. One of the advantages of isolating protein complexes from their physiological context in the living animal as compared with cells in culture is the possibility to reveal tissue-specific interactions that might not be present in heterologous cells. To explore this possibility, we compared the 14-3-3ζ binding partners identified by the TAP approach from brain (Table I) with the interactors obtained in HEK293 cells expressing TAP-14-3-3 (9). The HEK293 data includes a number of proteins that have been shown previously to interact with 14-3-3 proteins using other biochemical or cellular assays, such as kinesins; A-, B-, and C-murine sarcoma viral oncogene homolog (RAF) 1; Bcl2 antagonist of cell death (BAD); insulin receptor substrates (IRS1/4); cell division cycle (Cdc) 25; or histone deacetylase (HDAC)-4 and -5 (18–22). When compared with the 14-3-3ζ-associated proteins identified in transgenic brains, we found 22 common interactors, indicating that the characterization of protein complexes from transgenic mice is reliable. Almost 40 new interacting partners for 14-3-3ζ were identified by the transgenic method reflecting the importance of using a physiological environment for the identification of protein complexes.

Biochemical Validation of 14-3-3 Interactors

We selected some of the novel and brain-specific 14-3-3ζ binding partners from different protein classes for co-immu-

Fig. 1. **TAP from transgenic mice.** *A*, schematic representation of the DNA construct used for oocyte injection. *B*, the ubiquitin C promoter drives ubiquitous expression of TAP-14-3-3ζ. Western blot analysis using PAP antibody on total lysate from E12.5 embryos from a cross between the male founder line 540945 and a CD1 female mouse (*upper panel*). Genomic DNA from the yolk sacs was isolated and genotyped by PCR for presence of the transgene (*Ubi-NTAP*) or the Y chromosome (*Zfy*) (*lower panel*). *C*, TAP-14-3-3ζ expression in mouse adult tissues was monitored by Western blotting using PAP antibody. *D*, comparison of the levels of expression of the transgene (*TAP-14-3-3ζ*) with the endogenous 14-3-3 in control (wild-type (*WT*)) *versus* transgenic (*TG*) adult animals. 50 or 5 μg of protein from total brain lysates were analyzed by immunoblotting with PAP (*upper left panel*) or anti-pan-14-3-3 (*lower left panel*) antibodies. 50 μg of protein from liver and testis (*upper right panel*) and 100 μg of protein from different parts of the brain (*ob*, olfactory bulb; *hi*, hippocampus; *co*, neocortex; and *ce*, cerebellum) (*lower right panel*) were analyzed by immunoblotting with anti-pan-14-3-3. *E*, TAP-14-3-3ζ purification from transgenic mice. TAP-14-3-3ζ protein complexes were purified from transgenic brain, liver, and heart as indicated and stained with colloidal Coomassie. The TAP-14-3-3ζ is indicated with *black arrowheads*, while the positions of other 14-3-3 isotypes are indicated with *gray arrowheads*. The position in the gel of some other 14-3-3ζ-interacting partners discussed in this study is indicated with *arrows*.

TABLE I

Selected 14-3-3ζ-associated proteins identified by TAP-MS from transgenic mouse brains

Proteins were identified through a search of LC-MS/MS data against a combined human and mouse protein database, and the corresponding human proteins are listed according to their unique Human Genome Organisation (HUGO) gene symbols and National Center for Biotechnology Information (NCBI) gene ID. Domain composition obtained from SMART (Simple Modular Architecture Research Tool; dylan.embl-heidelberg.de/) and Pfam (Protein Family Database; pfam.wustl.edu/) is indicated. The absence (0) or the number (1–6) of consensus binding sites (CS) for 14-3-3 proteins are shown. UBA, ubiquitin-associated; RIIa, RIIα , regulatory subunit portion of type II PKA R-subunit; cNMP, cyclic nucleotide monophosphate-binding domain; ADK, adenylate kinase; RBD, ras-binding domain; C1, protein kinase C conserved region 1; STYKc, tyrosine kinase-like domain; PI4Kc, phosphoinositide 4-kinase, catalytic domain; IPK, inositol polyphosphate kinase; SAM, sterile α motif; DENN, differentially expressed in neoplastic *versus* normal cells; PH, pleckstrin homology domain; SH3, Src homology domain 3; RA, Ras association domain; RasGEF_N, GEF for Ras-like GTPases, N-terminal domain; RasGRF, Ras protein-specific guanine nucleotide-releasing factor domain; C2, protein kinase C conserved region 2; SEC14, Sec14p-like lipid-binding domain; ANK, ankyrin repeats; ArfGap, putative GTPase-activating proteins for the small GTPase ARF; IQ, calmodulin-binding motif; RasGEFN, GEF for Ras-like GTPases, N-terminal motif; VHP, Villin headpiece domain; CAP-Gly, cytoskeleton-associated proteins-Gly domain; KISc, kinesin motor domain; TPR, tetratricopeptide repeat domain; WH1, WASp homology domain 1; Iso_dh, isocitrate/isopropylmalate dehydrogenase; RING, Really Interesting New Gene domain; MIR, domain in ryanodine and inositol trisphosphate receptors and protein *O*-mannosyltransferases; RYDR_ITPR, RIH (RyR and IP3R homology) domain; BTB_POZ, BTB (for BR-C, ttk, and bab)/POZ (for pox virus and zinc finger) domain; K_tetra, K^+ channel tetramerization domain; Aldo_ket_red, aldo/keto reductase family; BRLZ, basic region leucin zipper.

Gene ID	Gene symbol	Description	Domains	CS
Signaling kinases				
17169	Mark3	Microtubule-associated protein/microtubule affinity-regulating kinase 3	Kinase domain, UBA domain	0
12322	*Camk2a*[a]	Calcium/calmodulin-dependent protein kinase (CaM kinase) IIα	Ser/Thr kinase domain	0
12323	Camk2b[a]	Calcium/calmodulin-dependent protein kinase (CaM kinase) IIβ	Ser/Thr kinase domain	0
12325	Camk2g[a]	Calcium/calmodulin-dependent protein kinase (CaM kinase) IIγ	Ser/Thr kinase domain	0
70661	BC033915[a]	Ser/Thr protein kinase	S_TKc	1
19088	Prkar2b[a]	cAMP-dependent protein kinase type II-β regulatory chain	RIIa, cNMP	0
229949	Ak5[a]	Adenylate kinase 5, ATP-AMP transphosphorylase	ADK	1
109880	Braf	v-*raf* murine sarcoma viral oncogene homolog B1	RBD, C1, STYKc	3
224020	*Pik4ca*[a]	Similar to phosphatidylinositol 4-kinase α	PI4Kc	1
228550	Itpka[a]	Inositol 1,4,5-trisphosphate 3-kinase A	IPK	0
Phosphatases, pseudophosphatases, and phosphodiesterases				
19047	Ppp1cc[a]	Protein phosphatase 1, catalytic subunit, γ isoform	PP2Ac	1
19052	Ppp2ca	Protein phosphatase 2 (formerly 2A), catalytic subunit, β isoform		0
51792	*Ppp2r1a*	Protein phosphatase 2, regulatory subunit A, α isoform	HEAT repeat	0
19057	*Ppp3cc*[a]	Protein phosphatase 3, catalytic subunit, γ isoform		0
53332	Mtmr1[a]	Myotubularin-related protein 1	TYR_phosphatase, GRAM	0
233977	Ppfia1	Protein-tyrosine phosphatase, interacting protein (liprin), α1	SAM	1
327814	*Ppfia2*[a]	Protein-tyrosine phosphatase, interacting protein (liprin), α2	SAM	2

TABLE I—*continued*

Gene ID	Gene symbol	Description	Domains	CS
68507	Ppfia4[a]	Protein-tyrosine phosphatase, interacting protein (liprin), α4	SAM	2
77980	Sbf1[a]	SET-binding factor	DENN, GRAM, PH	2
18573	Pde1a[a]	Calmodulin-dependent phosphodiesterase	PDEase	0
18578	Pde4b[a]	Phosphodiesterase 4B	PDEase	1
Signaling, small GTPase-related proteins				
16800	Arhgef2	Rho/Rac GEF2	PH, RhoGEF, C1	1
54126	*Arhgef7*	PIXB, Rho GEF7	SH3, RhoGEF, PH	1
102098	*Arhgef18*[a]	Rho/Rac GEF18; p114-Rho-GEF	RhoGEF, PH	2
76089	Rapgef2[a]	Rap GEF2 = PDZ-GEF1	cNMP_binding, PDZ, RA, RasGef_N, RasGRF	3
110279	Bcr[a]	GTPase-activating protein for p21rac	C2, PH, RhoGAP, RhoGEF	1
18015	Nf1[a]	Neurofibromin 1	RasGAP, SEC14	1
240057	Syngap1[a]	Synaptic Ras GTPase-activating protein 1 homolog	RasGAP, C2, PH	6
216963	Git1	G protein-coupled receptor kinase interactor 1	GIT1, ANK, ArfGap	1
19418	*Rasgrf2*[a]	Ras protein-specific guanine nucleotide-releasing factor 2	PH, IQ, RhoGEF, RasGEFN, RasGEF	2
228355	Madd[a]	Mitogen-activated protein kinase-activating death domain, (GDP/GTP exchange protein)	dDENN, DENN, uDENN	3
111173	Rab6ip2	Rab6-interacting protein 2	ELKS, Spectrin	1
52055	*Rab11fip5*[a]	GAF1, RAB11 family-interacting protein 5	C2 domain	4
Cytoskeleton-related proteins				
13829	Epb4.9[a]	Erythrocyte membrane protein band 4.9 (dematin)	VHP; Villin headpiece domain	2
269713	Cyln2[a]	Cytoplasmic linker 2	CAP-Gly	0
16573	Kif5b	Kinesin family member 5B	KISc domain	0
16574	*Kif5c*	Kinesin family member 5C	KISc domain	0
16593	*Kns2*	Kinesin 2 (60–70 kDa); kinesin light chain 1	4 TPR repeats	0
16594	*Klc2*	Likely ortholog of kinesin light chain 2 (FLJ12387)	5 TPR repeats	1
Signaling adaptor proteins				
7534	*YWHAZ*	14-3-3ζ		
54401	*Ywhab*	14-3-3β/α		
22627	*Ywhae*	14-3-3ϵ		
22629	*Ywhah*	14-3-3η		

noprecipitation in HeLa cells. (i) AK5 has a restricted expression in brain and catalyzes the reversible phosphorylation between nucleoside triphosphates and monophosphates (23). (ii) LDB1 is a ubiquitous nuclear, multiadaptor protein originally identified as a cofactor for LIM homeodomains and LIM domain only (LMO) proteins. Targeting of *Lbd1* in mice revealed a role in neuronal patterning and development (24). (iii) PDE1A, a Ca^{2+}/calmodulin-stimulated 3′,5′-cyclic nucleotide phosphodiesterase, is a membrane-bound exonuclease that hydrolyzes phosphodiester bonds (25). (iv) MADD is an adaptor protein that binds to tumor necrosis factor receptor 1 and regulates the recycling of Rab3 small GTPase proteins that have an essential role in Ca^{2+}-dependent neurotransmitter release and exocytosis (26). (v) SWI/SNF-related matrix-associated actin-dependent regulator of chromatin subfamily B1 (SMARCB1) is a member of the chromatin-remodeling SWI/SNF complex (27). SMARCB1 is required for retroviral integration (28), and mutations in its gene predispose an individual to a variety of cancers (29).

The corresponding cDNAs were cloned as CFP fusion pro-

TABLE I—*continued*

Gene ID	Gene symbol	Description	Domains	CS
22628	*Ywhag*	14-3-3γ		
22630	*Ywhaq*	14-3-3τ		
26558	*Homer3*	Regulate group 1 metabotropic glutamate receptor function	WH1	0
Metabolism, homeostasis				
18640	*Pfkfb2*	6-Phosphofructo-2-kinase/ fructose-2,6-bisphosphatase 2	6-Fructo kinase domain	1
13808	*Eno3*[a]	Enolase 3; 2-phospho-D-glycerate hydrolyase		0
170718	Idh3b[a]	NAD^+-dependent isocitrate dehydrogenase	Iso_dh	0
Cellular and vesicle trafficking				
55992	Trim3[a]	Tripartite motif-containing 3	B-box-type zinc finger, RING finger, filamin-type immunoglobulin domains	2
26949	Vat1[a]	Vesicle amine transport protein 1 homolog		0
Ion channel, transport carrier				
16438	Itpr1[a]	Inositol 1,4,5-trisphosphate receptor, type 1	MIR, RYDR_IPTR	0
383348	Kctd16[a]	Potassium channel tetramerization domain-containing 16	BTB_POZ, K_tetra	0
16498	Kcnab2[a]	Potassium voltage-gated channel, β member 2	Aldo/ket_red	1
Transcription, chromatin structure				
16825	Ldb1[a]	LIM domain binding 1		0
93760	Arid1a[a]	SMARCF1; chromatin-remodeling factor p250		2
20587	Smarcb1[a]	SWI/SNF-related, SNF5 homolog	SNF5 domain	2
Miscellaneous				
108686	A430106J12Rik[a]	Peptidase activity	BRLZ	2
66049	Rogdi[a]	Leucine zipper domain protein	Leucine zipper domain	0

[a] Protein specifically interacting in brain.

teins and expressed alone or together with HA epitope-tagged 14-3-3ζ (HA-14-3-3ζ)) in HeLa cells. Co-immunoprecipitation studies confirmed the association of 14-3-3ζ with AK5, LDB1, PDE1A, and MADD (Fig. 2, *A–D*). Subcellular fractionation showed that CFP-SMARCB1 is associated with HA-14-3-3ζ specifically in the cytosol but not in the nucleus (Fig. 2*E*).

Co-immunopreciptiation Analysis of Interactions between MARK2, MARK3, MARK4, and 14-3-3ζ, -η, -β, and -γ Isotypes

A number of 14-3-3ζ-associated proteins were not found with TAP-14-3-3β, -14-3-3η, or -14-3-3γ (Ref. 9 and data not shown). Specificity of interaction of a subset of ligands binding to different 14-3-3 isotypes with different affinities has been shown previously (30). However, a detailed analysis of 14-3-3 isotype specificity is still poorly documented. Therefore, we addressed the specificity of interactions between a family of related kinases, the microtubule-associated protein/microtubule affinity-regulating kinases (MARKs) and different 14-3-3 isotypes. MARK3 is a member of the serine protein kinase subfamily, also including MARK1, -2, and -4, that phosphorylates substrates and thereby induces binding to 14-3-3 proteins (31). MARK3 was identified as an interacting partner of 14-3-3ζ both in mouse brain (Table I) and in cells in culture (data not shown and Ref. 7). To address the specificity of the MARK/14-3-3 association, different MARK family members were transiently expressed in the presence of different 14-3-3 isotypes. The binding specificity was then assessed by co-immunoprecipitation in HEK293 cells using HA- and Myc-tagged proteins. Fig. 3 shows the interaction specificities between the MARK family members and the 14-3-3 isotypes. 14-3-3ζ interacted with MARK3 but not or only very weakly with MARK2 (Fig. 3*A*). In contrast, no 14-3-3ζ-MARK4 association could be detected (Fig. 3*A*). 14-3-3β and 14-3-3γ strongly interacted with MARK3 and to a lesser extent with MARK2 but not with MARK4, whereas 14-3-3η interacted

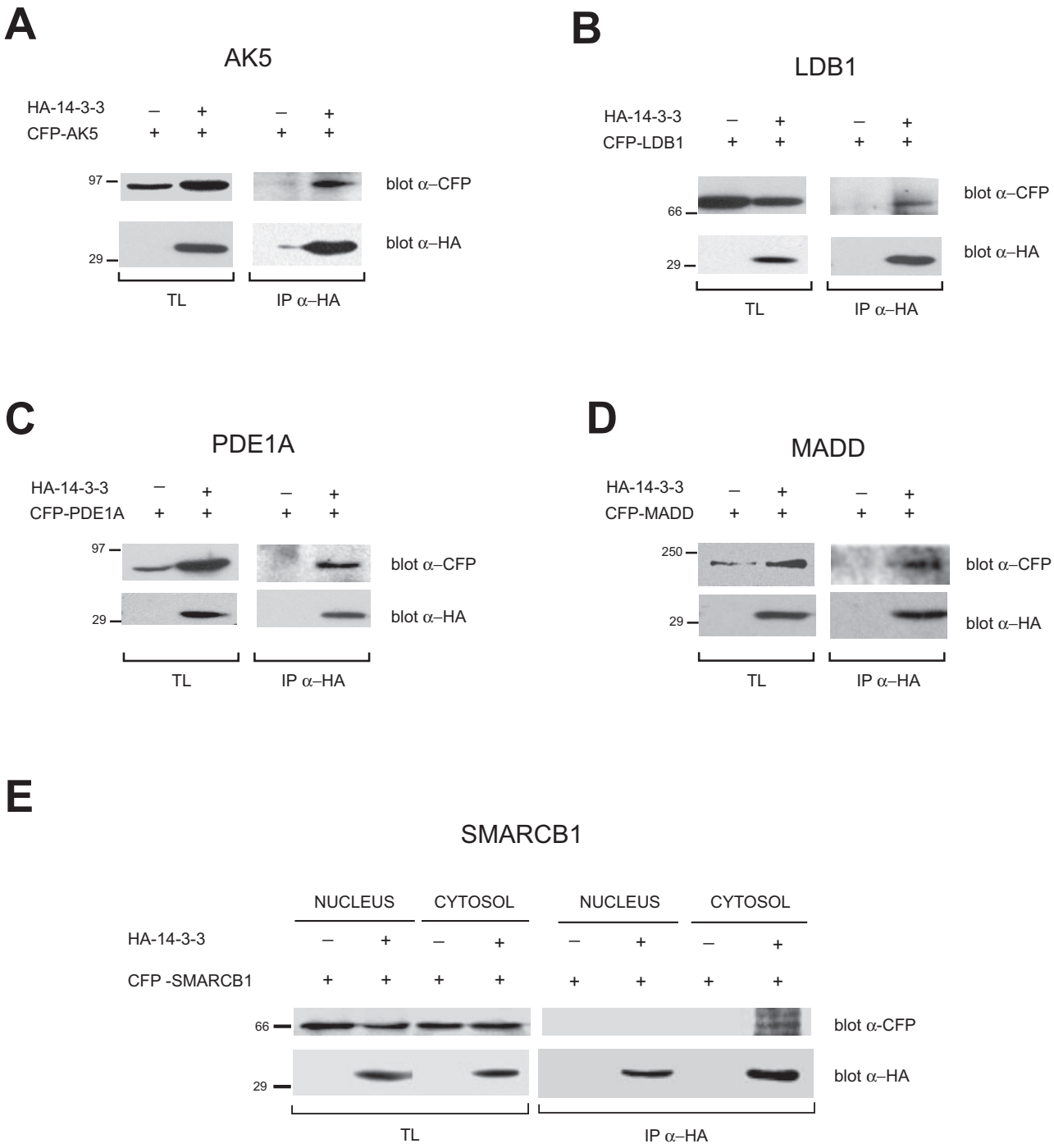

FIG. 2. **Co-immunoprecipitation experiments confirm the association of 14-3-3ζ with several novel partners identified from transgenic mouse proteomics in brain.** *A–D*, HeLa cells were transfected with CFP-tagged AK5 (*A*), LDB1 (*B*), PDE1A (*C*), or MADD (*D*) alone or together with HA-14-3-3ζ. Levels of transfection in total lysates (*TL*) and HA immunoprecipitates (*IP α-HA*) were analyzed by SDS-PAGE followed by Western blotting with the indicated antibodies. *E*, 14-3-3ζ binds specifically to the cytosolic subpopulation of SMARCB1. HeLa cells expressing CFP-SMARCB1 alone or together with HA-14-3-3ζ were subjected to cytosolic and nuclear fractionation. HA immunoprecipitates and total lysates were analyzed by immunoblotting with the indicated antibodies.

with all three MARK proteins (Fig. 3, *B–D*). Thus co-immunoprecipitation experiments indicating specificity of binding between MARK and 14-3-3 proteins corroborated the TAP-MS experiments using TAP-14-3-3ζ from both transgenic brains and HEK293 cells, whereas MARK3 and MARK2 were identified when TAP-14-3-3γ was used as a bait (data not shown and Ref. 8), and MARK2, -3, and -4 were recovered with TAP-14-3-3η (9).

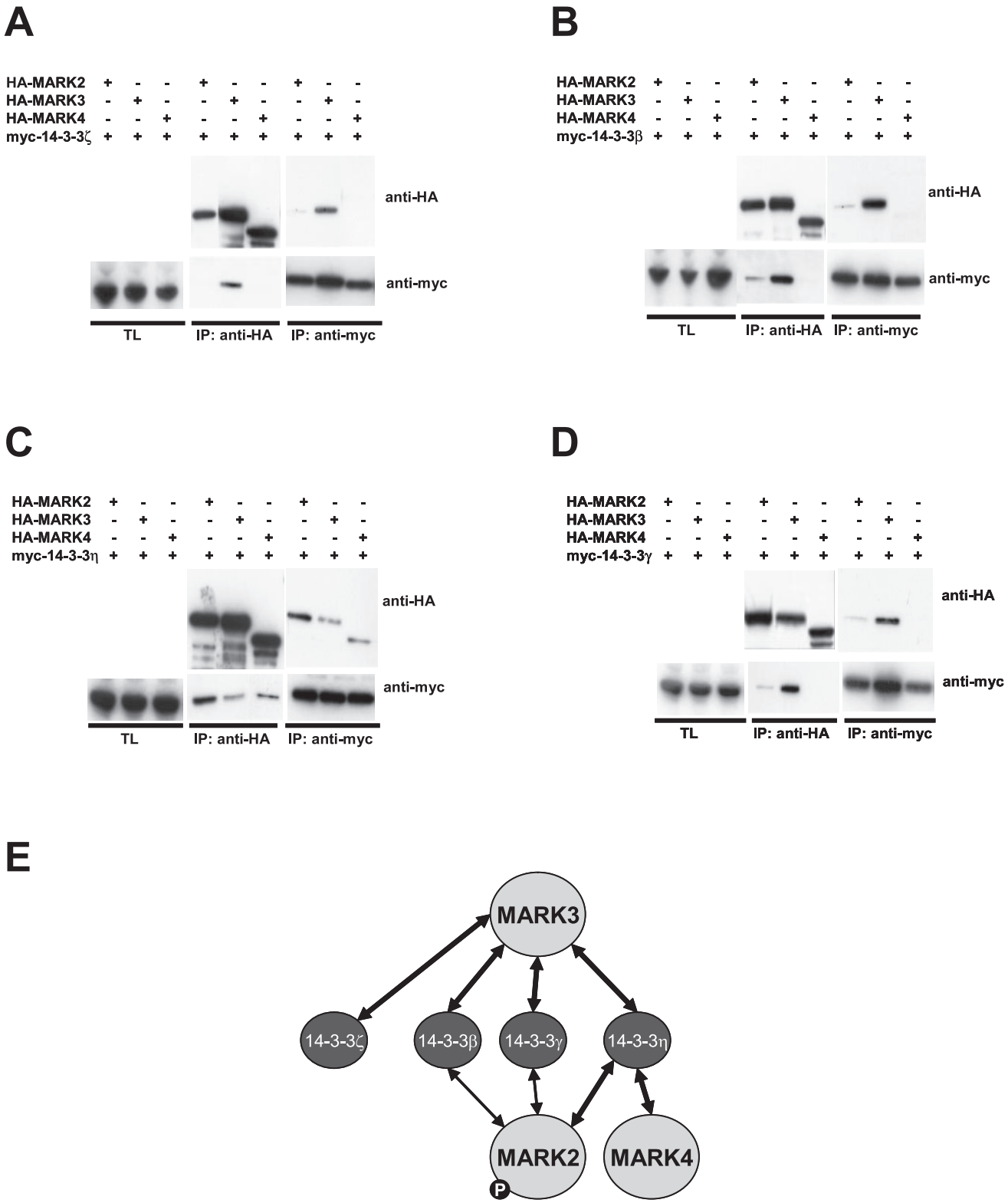

FIG. 3. **Specificity of binding to different 14-3-3 isoforms.** *A–D*, co-immunoprecipitation analysis of interactions between MARK2, MARK3, MARK4, and the 14-3-3ζ, 14-3-3β, 14-3-3η, and 14-3-3γ isotypes. HEK293 cells were transfected to express transiently the different HA-tagged MARK isotypes and Myc-tagged 14-3-3ζ (*A*), 14-3-3β (*B*), 14-3-3η (*C*), and 14-3-3γ (*D*). Proteins were immunoprecipitated (*IP*) and detected by immunoblotting using the indicated antibodies. *E*, schematic representation of the co-immunoprecipitation studies performed in *A–D*. The strength of the interactions is indicated by the *thickness* of the *arrows*. *P* indicates that the corresponding protein contains a putative binding site for 14-3-3 proteins. *TL*, total lysates.

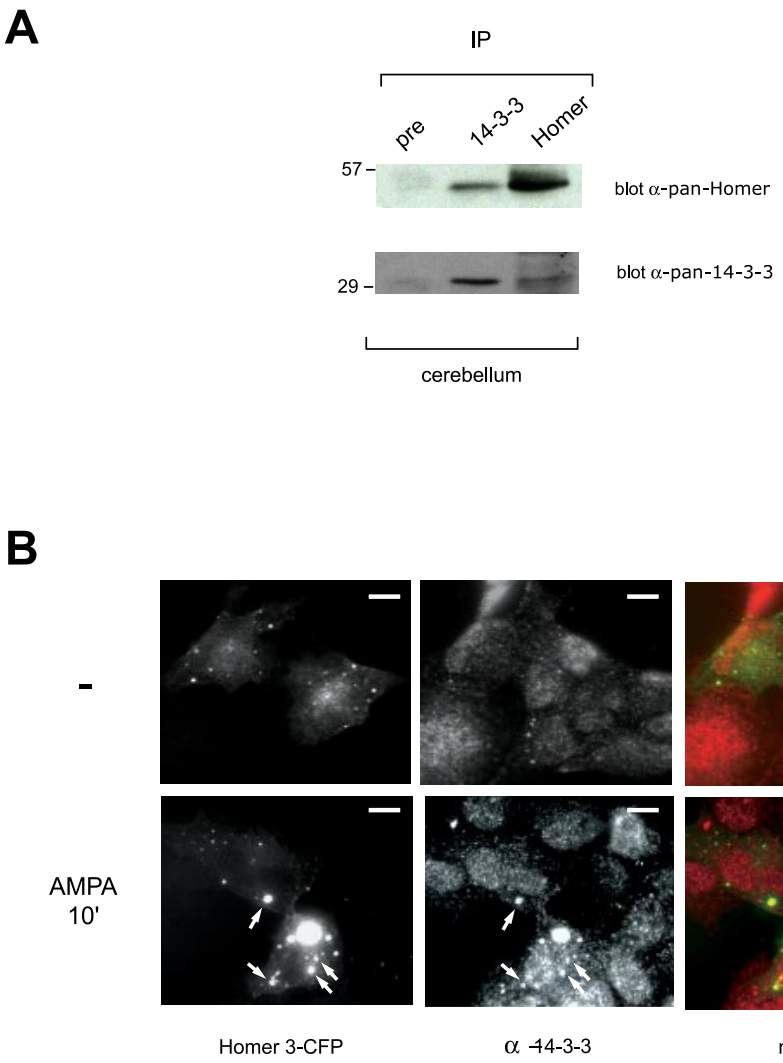

FIG. 4. **Endogenous 14-3-3 proteins associate with Homer *in vivo* and relocalize in response to AMPA receptor stimulation.** *A*, 14-3-3 proteins interact with Homer in the murine cerebellum. Lysates from adult mice cerebellum were immunoprecipitated (*IP*) with rat preimmune serum (*pre*), anti-pan-14-3-3, or anti-pan-Homer antibodies. Immunoprecipitates were separated and analyzed by Western blotting with the indicated antibodies. *B*, interaction of 14-3-3 and Homer 3 is regulated by AMPA receptor stimulation. SK-N-BE(2) cells were transiently transfected to express CFP-Homer 3. Cells were untreated (*upper panels*) or stimulated (*lower panels*) with AMPA for 10 min (*10′*). The *right column* shows the merge of the two signals with CFP in *green* for Homer 3 (*left column*) and anti-14-3-3 staining in *red* for endogenous 14-3-3 proteins (*middle column*). *Arrows* indicate places of Homer 3 accumulation and recruitment of endogenous 14-3-3 proteins. *Scale bar*, 10 μm.

In Vivo 14-3-3 Protein Associations Revealed New Functions for 14-3-3 Proteins in Cellular Signaling and Modulation of the Cytoskeleton

We next investigated whether 14-3-3 binding to some of its associated proteins would modulate their subcellular distribution and activity in response to cellular signaling and the physiological role of such interactions. We focused on the function of 14-3-3 binding to Homer 3, βPIX, and GIT1.

14-3-3 Distribution Responds to Glutamate Receptor Transduction via Association with Homer 3—Homer family members are postsynaptic adaptors harboring distinct regional, cellular, and subcellular patterning during postnatal brain development with Homer 3 mainly restricted to the cerebellum (32). To investigate the association of 14-3-3 and Homer proteins in the adult mouse brain, we performed co-immunoprecipitations using specific antibodies. Fig. 4*A* shows that the endogenous 14-3-3 proteins and Homer indeed interact *in vivo* in the adult mouse cerebellum.

Homer 3 is a postsynaptic density scaffolding protein that links multiple targets involved in glutamate receptor signaling (33). In particular, Homer proteins bind directly to metabotropic glutamate receptors type I (mGluR1 and mGluR5) and to SH3 (Src homology 3) and multiple ankyrin repeat domains (Shank) proteins, forming a higher order protein complex that cross-links mGluRs with *N*-methyl-D-aspartate receptors. Fig. 4*B* shows that the stimulation of the AMPA receptors with AMPA in SK-N-BE(2) neuroblastoma cells led to the clustering of exogenous CFP-Homer 3 in big patches at the membrane. This redistribution of Homer 3, presumably due to its association with endogenous proteins involved in the AMPA receptor activation downstream cascade, correlates with the recruitment of endogenous 14-3-3 proteins to the same large patches and suggests that 14-3-3 interactions respond to glutamate receptor signaling.

14-3-3ζ Modulates the Activity of Associated GIT-PIX Partners Involved in Cytoskeleton Rearrangements—Structural rearrangements of the actin cytoskeleton in response to external signals are triggered through diverse cell surface

receptors, and all of these signals converge inside the cell on a group of small monomeric GTPases that are members of the Rho protein family (Cdc42, Rac, and Rho). These GTPases cycle between active GTP-bound and inactive GDP-bound forms, and their activation requires the action of guanine nucleotide exchange factors (GEFs) to promote the conversion of the GDP to the GTP state. The PIX family members (αPIX/ARHGEF6 and βPIX/ARHGEF7) are GEFs for Rac1 and Cdc42 small GTPases. GIT proteins have been reported to directly homo- and heterodimerize and interact with PIX proteins through at least two distinct sites (34). Moreover GIT-PIX complexes have been shown to be recruited to numerous cellular locations through distinct protein-protein interactions (34). Our analysis revealed that several members of the GIT-PIX complex, like βPIX and GIT1, were found to associate with 14-3-3ζ (Table I). Binding of βPIX and GIT1 to 14-3-3ζ was first confirmed by co-transfection experiments in HeLa cells (data not shown). Co-immunoprecipitation studies from adult mouse brain lysates with specific anti-βPIX antibodies confirmed that βPIX forms *in vivo* a complex with 14-3-3 proteins (Fig. 5*A*). In the reverse experiment, GIT1 and to a lesser extent PIX proteins were co-immunoprecipitated by 14-3-3-specific antibodies (Fig. 5*A*). Moreover the GIT1 proteins immunoprecipitated from adult mouse brain showed immunoreactivity to a phosphoserine 14-3-3 binding motif suggesting that GIT1 contains a phosphorylated motif that could bind directly to 14-3-3 (Fig. 5*B*).

Individual members of the Rho family are known to cause specific changes to the actin cytoskeleton; the activation of Cdc42 triggers actin polymerization and bundling to form either filopodia or shorter cell protrusions called microspikes, whereas the activation of Rac1 promotes actin polymerization at the cell periphery leading to the formation of sheetlike lamellipodial extensions and membrane ruffles. To test the functional implication of the βPIX and 14-3-3ζ interaction on the cytoskeletal rearrangements induced by βPIX, YFP-tagged 14-3-3ζ (YFP-14-3-3ζ) and CFP-βPIX were transiently overexpressed in HeLa cells, and the actin filaments were labeled with fluorescent phalloidin (Fig. 5, *C–H*). Transfection of HeLa cells with βPIX led to activation of Rac (Fig. 5*J*) and the consequent formation of lamellipodia (Fig. 5, *E* and *I*). Co-expression of 14-3-3ζ and βPIX increased the βPIX-induced Rac activity (Fig. 5*J*) as well as lamellipodia and membrane ruffle formation (Fig. 5, *F* and *I*) suggesting that the binding of 14-3-3ζ increases the activity of βPIX. To further investigate the role of 14-3-3ζ in lamellipodia and membrane ruffle formation, a dominant negative form of 14-3-3ζ (14-3-3ζ-DN) able to homo- and heterodimerize but not able to interact with target proteins was used (12). Remarkably co-expression of YFP-14-3-3ζ-DN and CFP-βPIX not only abolished lamellipodia formation (Fig. 5, *G* and *I*) but also induced filopodia formation (Fig. 5*G*) and increased the Cdc42 activity (Fig. 5*J*) suggesting a shift of βPIX GEF activity toward Cdc42 activation. Transfection of 14-3-3ζ-DN alone did not promote filopodia formation in these cells (Fig. 5*H*).

The GIT1-βPIX complex is also involved in spine morphology and synapse formation (35). To investigate whether the interaction between 14-3-3ζ and βPIX could be involved in such a biological process, E18 rat hippocampal neurons DIV7 (7 days *in vitro*) were co-transfected with constructs expressing Myc-βPIX and/or YFP-14-3-3ζ. 7 days later, when the dendritic arbor was organized, neurons were fixed, and protrusions were analyzed (Fig. 6). Spines in cultured hippocampal neurons are observed to form between DIV7 and DIV14. By DIV14 most dendritic protrusions are spines; however, their maturation continues until DIV21. Spine morphogenesis in YFP-transfected cultures was characterized by a decrease in spine length and formation of mature mushroom-like heads (Fig. 6, *A* and *G*). As expected, in βPIX-transfected neurons, we detected numerous long, thin filopodia-like protrusions without heads (Fig. 6, *C*, *E*, *F*, and *G*). These dendritic protrusions are the result of the mislocalization of βPIX, which in turn distributes diffusely active Rac1 in the entire neuron leading to an increase of these filopodia-like protrusions (35). Interestingly expression of YFP-14-3-3ζ in hippocampal neurons had a dramatic effect on spine formation. 14-3-3ζ-overexpressing neurons presented a particularly high number of mature spines with mushroom-like heads, covering in some cases the entire dendrite (Fig. 6, *B*, *E*, and *F*). The presence of 14-3-3ζ increased the density of mature spines by 40% compared with control YFP-transfected neurons (Fig. 6*F*). This suggests that 14-3-3ζ is a potent regulator of spine growth, inducing the maturation of filopodia to mushroom-like short protrusions. Co-transfection of 14-3-3ζ with βPIX did not change the total number of protrusions in the dendrites (Fig. 6*E*) but increased significantly the number of protrusions with heads in comparison to βPIX alone (see *arrows* in Fig. 6*D* and quantification in Fig. 6, *E* and *F*) suggesting that 14-3-3 is a potent spine maturation regulator. The protrusions in the double 14-3-3ζ- and βPIX-transfected neurons had mature heads independent of the length of the protrusion. These results suggest that 14-3-3ζ could stabilize and mature the long filopodia induced by βPIX activity and point out an interesting role of 14-3-3 proteins in regulating spine morphology.

DISCUSSION

Most cellular processes require protein-protein interactions or the assemblies of large complexes of proteins. Supplementing genetic approaches, the study of such protein-protein interactions has emerged as a valuable method for unraveling signaling pathways and cellular processes. Recent advances in mass spectrometry have made possible the identification of multisubunit protein complexes isolated from cell lysates with high sensitivity and accuracy. A method to isolate native protein complexes from cells is the key requirement for these proteomics analyses. The TAP technology when coupled to MS has proven to efficiently permit the characterization of protein complexes from *Escherichia coli*, yeast, and

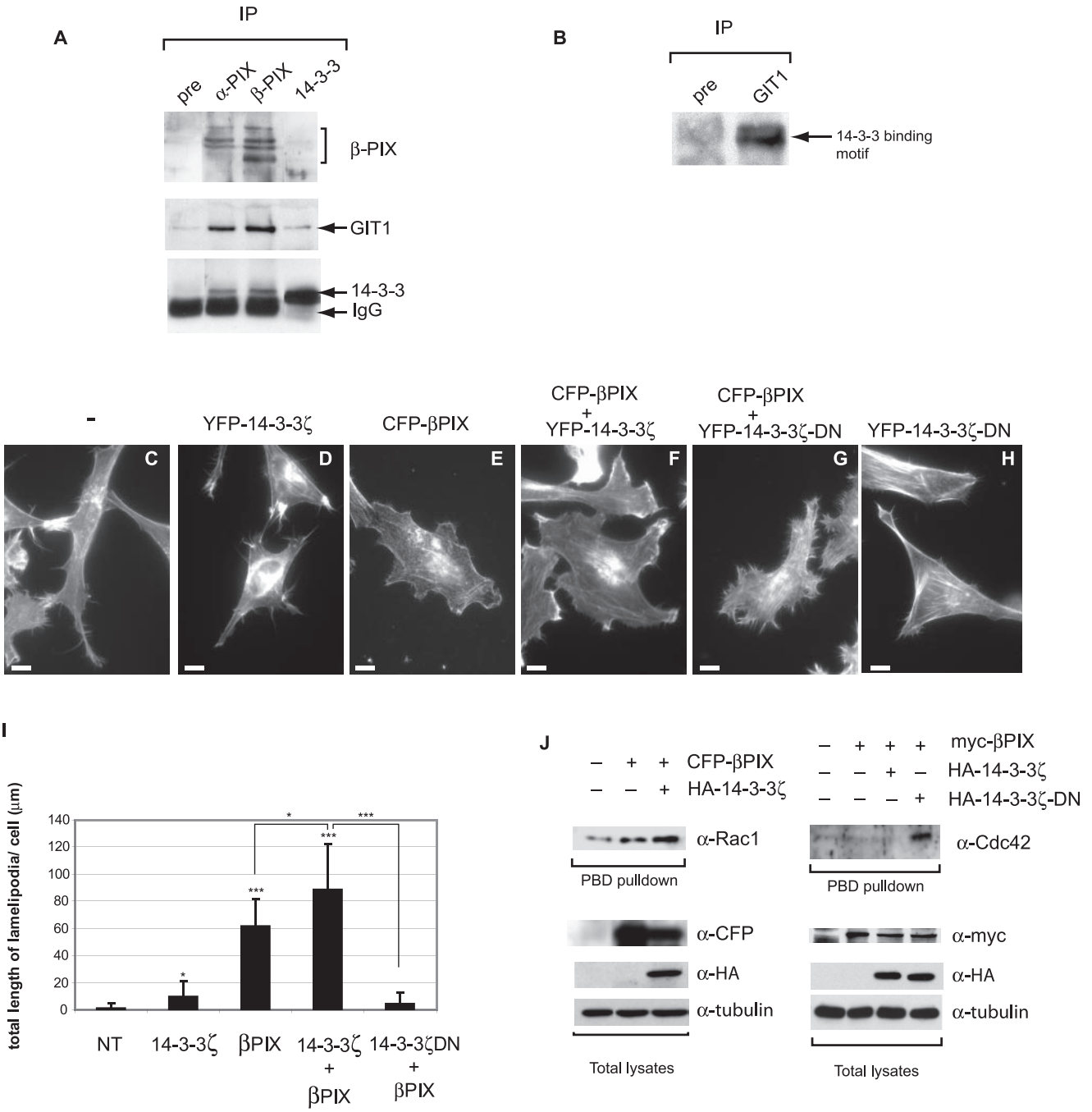

FIG. 5. **14-3-3 binding to βPIX regulates cytoskeleton rearrangements.** *A*, 14-3-3 forms multiprotein complexes *in vivo* with GIT1, αPIX and βPIX in mouse brain. Murine brain lysates were immunoprecipitated (*IP*) with rabbit preimmune serum (*pre*) or the indicated antibodies and analyzed by immunoblotting. *B*, GIT1 contains a phospho-Ser 14-3-3 binding motif. Murine brain lysates were immunoprecipitated with the indicated antibodies and analyzed by Western blotting with phospho-Ser 14-3-3 binding motif antibody. *C–H*, interaction of 14-3-3 and βPIX increases the lamellipodia and membrane ruffle formation induced by βPIX. HeLa cells growing on laminin were transfected with YFP-14-3-3ζ (*D*), CFP-βPIX (*E*), CFP-βPIX and YFP-14-3-3ζ (*F*), CFP-βPIX together with the dominant negative YFP-14-3-3ζ-DN (*G*), or the dominant negative YFP-14-3-3ζ-DN alone (*H*). Actin filaments were stained with Texas Red-conjugated phalloidin. *Scale bar*, 10 μm. *I*, quantification of the lamellipodia and membrane ruffle formation in the different conditions shown in *C–G*. The length of lamellipodia per cell is shown. The graph is a representative experiment of five different experiments ($n = 60$ cells/experiment). *Bars* represent S.E. from one experiment. *, $p < 0.05$; ***, $p < 0.0005$ with *t* test compared with the non-transfected (*NT*) control or between samples as indicated. *J*, binding of 14-3-3 to βPIX stimulates the βPIX-induced Rac activity in HeLa cells, whereas the dominant negative 14-3-3 causes a shift to an increased Cdc42 activity. The Rac (*left panels*) and Cdc42 (*right panels*) exchange activity of βPIX expressed in HeLa cells alone and together with 14-3-3ζ or 14-3-3ζ-DN was measured by p21-activated protein binding domain (*PBD*) pulldown. Levels of the transfected proteins as well as tubulin for loading control were detected by immunoblotting with the indicated antibodies.

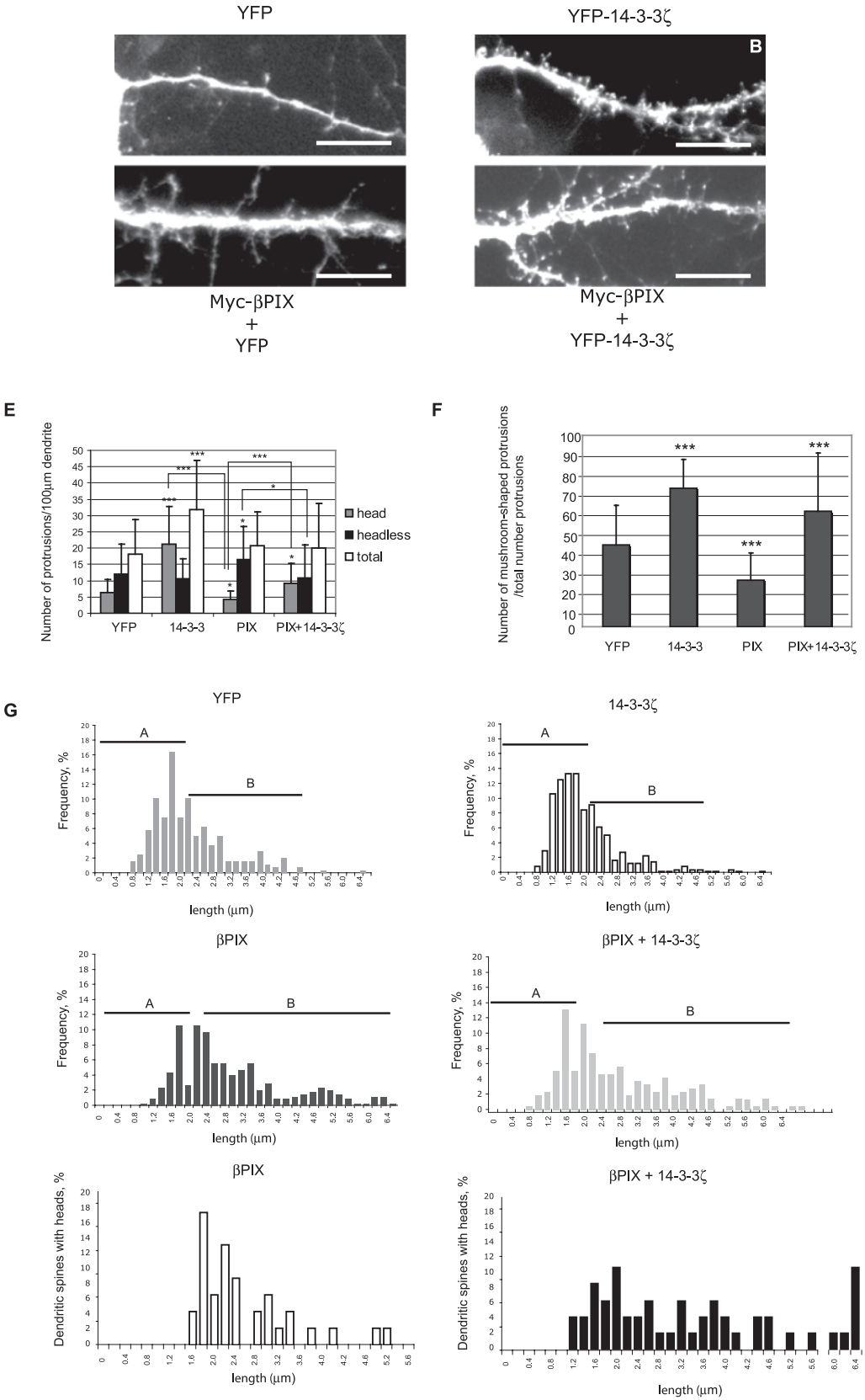

mammalian cells in culture as well as from multicellular organisms such as *Caenorhabditis elegans* or *Drosophila melanogaster* (for a review, see Ref. 36). The present study represents the first application of the TAP-MS technology to the mouse and opens the way to the study of tissue-specific or cell type-specific protein complexes.

Vectors based on the human ubiquitin C promoter were constructed to drive ubiquitous expression of TAP-tagged proteins in transgenic mice. Protein complexes were purified, and analysis of the resulting protein mixtures revealed expected known associated proteins. Consistent with the ability of 14-3-3 proteins to form homo- and heterodimers, most of the other 14-3-3 isotypes were purified from transgenic brains, livers, and hearts expressing TAP-14-3-3ζ (liver and heart data not shown). We conclude from this that TAP-MS can be used for studying the mouse proteome *in vivo*. In the case of the samples from brain, around 60 proteins were detected to be associated with TAP-14-3-3ζ, and 61% of them were not previously described, pointing to the relevance of using specific tissues for the isolation of complexes. Interestingly the advantage of the TAP transgenic mice is the possibility to study putative different binding partners of a certain protein at different developmental stages.

To demonstrate that TAP-MS from transgenic mice provides additional information when compared with a proteomics approach using cells in culture, we compared the dataset against a dataset that we generated from HEK293 cells expressing different isoforms of TAP-tagged 14-3-3 (9). During the course of the study, three independent proteomics reports on 14-3-3 proteins were published. Jin *et al.* (8) used a similar approach where a FLAG-tagged 14-3-3γ protein was expressed in HEK293 cells, whereas others have used the *in vitro* binding of human HeLa cell proteins to immobilized homologous 14-3-3 proteins from yeast BMH1 and BMH2 (6) or mammalian 14-3-3ζ (7). Around 33% of the 14-3-3ζ-binding proteins revealed by transgenic mouse proteomics from brain were also identified from cells in culture systems using TAP-14-3-3η (9) or TAP-14-3-3ζ, TAP-14-3-3β, and TAP-14-3-3γ (data not shown). However, a high number of proteins were identified as brain-specific 14-3-3ζ binding partners either because they are specifically expressed in brain (*i.e.* AK5) or the activation state allows their specific interaction with 14-3-3 proteins in this tissue.

We were able to confirm using co-immunoprecipitation assays with different tags the association of five of these new targets (AK5, LDB1, PDE1A, MADD, and SMARCB1) not previously identified in our cell culture models or in the other proteomic descriptions with 14-3-3 proteins as well as Homer 3, detected in brain and in our cell culture models, and MARK3, GIT1, and βPIX, which have also been shown previously to interact with other 14-3-3 isoforms (6–8). From these proteins chosen for further biochemical characterization only MADD, GIT1, βPIX, AK5, and SMARCB1 contain consensus sequences for 14-3-3 binding. Interestingly GIT1 showed immunoreactivity with an antibody developed to recognize phosphorylated consensus sequences in 14-3-3 binding partners. However, PDE1A, LDB1, MARK3, and Homer 3 do not contain any 14-3-3 binding consensus sequence suggesting that these proteins could bind indirectly to 14-3-3 or through a non-consensus sequence. In the case of MARK3, it has been reported that it can interact indirectly with 14-3-3 via specific substrates like kinase suppressor of Ras 1 (KSR1) (37).

14-3-3 proteins have been implicated in the regulation of the subcellular localization of many phosphorylated target proteins and in particular in the trafficking between the nucleus and the cytoplasm. Often nuclear proteins become phosphorylated and through the binding to 14-3-3 accumulate in the cytoplasm (for a review, see Ref. 1). Here we describe the binding of 14-3-3 to a member of the chromatin-remodeling SWI/SNF multiprotein complexes, SMARCB1, exclusively in the cytosol. We speculate that SMARCB1 could be retained in the cytoplasm depending on the activity of the 14-3-3 anchoring protein as it has been described for the cyclin-dependent kinase inhibitor p27(Kip1) (38) or the histone deacetylases HDAC4 and HDAC5 (21).

With many binding partners of 14-3-3 identified in this and other studies, it becomes very important to characterize in detail such interactions and their functional consequences. We studied in more detail the interactions between 14-3-3ζ and different proteins identified in our proteomics approach: βPIX, GIT1, and Homer 3. Using specific antibodies, we could show that endogenous βPIX, GIT1, and Homer associate with endogenous 14-3-3 proteins in the adult mouse brain, and such interactions play various, not previously described cellular roles.

Fig. 6. **14-3-3 induces the maturation of spines in cultured rat hippocampal neurons.** *A–D*, E18 rat hippocampal neurons were transfected at DIV7 with YFP (*A*), YFP-14-3-3ζ (*B*), Myc-βPIX together with YFP (*C*), or YFP-14-3-3ζ (*D*). 7 days after the transfection, the neurons were fixed, and the spine formation was analyzed by immunofluorescence. Dendrites are shown in the YFP channel. *Arrows* point to unusual long filopodia with mushroom-like heads. *Scale bar*, 10 μm. *E*, quantitative analysis of spine density analyzed by counting the number of total protrusions, with heads and headless, in 100 μm of a dendrite ($n > 100$ dendrites). *F*, quantitative analysis of spine maturation. The percentage of mature mushroom-like spines relative to total number of protrusions is represented ($n > 100$ dendrites). *G*, quantitative analysis of the lengths of dendritic protrusions ($n > 500$) analyzed for each transfection condition: YFP (*left upper panel*), 14-3-3ζ (*right upper panel*), Myc-βPIX (*left middle panel*), and Myc-βPIX + YFP-14-3-3ζ (*right middle panel*). *Group A* represents spines, and *group B* represents dendritic filopodia based on the length. The length of exclusively protrusions with heads is also represented for the transfections with Myc-βPIX (*left bottom panel*) and Myc-βPIX + YFP-14-3-3ζ (*right bottom panel*).*, $p < 0.05$; ***, $p < 0.0005$ with *t* test compared with the YFP control or between samples as indicated.

We have now implicated 14-3-3 proteins in glutamate receptor signaling because there was a redistribution of 14-3-3 proteins after AMPA receptor stimulation in SK-N-BE(2) neuroblastoma cells. In addition to binding Homer proteins, Shank proteins have also been shown to bind glutamate receptor-interacting protein 1 (GRIP1) (39), a PDZ-containing protein that binds to AMPA receptors, and therefore Homer-Shank-GRIP1 complex constitutes a bridge that allows the physical and functional association between mGluRs type I and AMPA receptors. The fact that we found a clustering of Homer3 and 14-3-3 proteins and that we have found 14-3-3 associated to GRIP1-TAP in HEK293 cells (data not shown) suggests that 14-3-3 proteins could be regulating the formation of a protein complex downstream of mGluRs type I and AMPA receptors.

14-3-3 binding to GIT1 and βPIX regulated cytoskeleton dynamics in HeLa cells, increasing lamellipodia and membrane ruffle formation. A dominant negative form of 14-3-3 not able to interact with target proteins, however, induced filopodia formation. It has been shown that the αPIX GEF activity is tightly coupled to its monomer-dimer equilibrium: the dimeric form of αPIX functions as a Rac-specific GEF, whereas the monomeric αPIX is a GEF for Cdc42 (40). Because the domains involved in the dimerization of PIX proteins and in the Rac/Cdc42 activation are conserved, we propose that βPIX could be subjected to the same mechanism of regulation. 14-3-3 binding could then stimulate the dimeric form and activate primarily Rac and therefore increase lamellipodia and membrane ruffle formation, whereas a dominant negative form of 14-3-3 will shift the equilibrium to a monomeric form, *i.e.* to Cdc42 activation and filopodia formation.

Finally our biochemical and functional analysis indicated as well a very interesting new role for 14-3-3 proteins in spine morphology and synapse formation in neurons. The molecular mechanisms of spine formation are poorly understood. An immature neuron has dendritic filopodia that constitute a sensing element in the formation of synaptic contacts with adjacent neurons. These filopodia are cytoplasmic protrusions 2–10 μm long and less than 1 μm thick that after presynaptic contact collapse to become a short, 1–2-μm, "mature" spine (41). Localized Rac activity induced by the GIT1-βPIX complex has been shown to be essential for filopodia formation (35). We have shown now that 14-3-3 proteins could be involved in the process of spine formation by inducing the maturation of the filopodial dendritic extensions. Consistent with this role, overexpression of 14-3-3 increased dramatically the spine density in hippocampal neurons.

In conclusion, by identifying novel 14-3-3ζ interactors, the proteomics approach applied to mouse brain has given significant new insights to the role that 14-3-3 proteins play in several new biological processes, such as AMPA signaling and actin cytoskeleton rearrangements. The TAP-MS method developed in transgenic mice turns out to be a powerful approach to study the mouse proteome *in vivo* and offers the exciting possibility to study in the future tissue- or developmental stage-specific protein complexes.

Acknowledgments—We thank A. Walling, T. Weiss, S. Weinges, J. Egea, E. Kramer, and G. Wilkinson (Max Planck Institute, Munich, Germany) as well as all members of the Cellzome Mass Spectrometry and Information Technology groups for outstanding technical expertise and diligence. We thank R. Premont for providing the cDNAs and antibodies for GIT1 and PIX.

* The costs of publication of this article were defrayed in part by the payment of page charges. This article must therefore be hereby marked "*advertisement*" in accordance with 18 U.S.C. Section 1734 solely to indicate this fact.

[S] The on-line version of this article (available at http://www.mcponline.org) contains supplemental material.

§ Present address: Interdisciplinary Research Institute, Inst. de Biologie de Lille, 1 rue du Pr. Calmette, F-59021 Lille cedex, France.

¶ To whom correspondence may be addressed. E-mail: pierre-olivier.angrand@ibl.fr.

** Present address: Genentech Inc., 1 DNA Way, South San Francisco, CA 94080.

§§ Present address: Samuel Lunenfeld Research Inst., Mount Sinai Hospital, 600 University Ave., Toronto, Ontario M5G 1X5, Canada.

¶¶ Present address: Center for Molecular Medicine of the Austrian Academy of Sciences, Lazarettgasse 19/3, 1090 Vienna, Austria.

‖‖ To whom correspondence may be addressed. Tel.: 49-89-8578-3159; Fax: 49-89-8578-3152; E-mail: palmer@neuro.mpg.de.

REFERENCES

1. MacKintosh, C. (2004) Dynamic interactions between 14-3-3s and phosphoproteins regulate diverse cellular processes. *Biochem. J.* **381,** 329–342
2. Muslin, A. J., Tanner, J. W., Allen, P. M., and Shaw, A. S. (1996) Interaction of 14-3-3 with signaling proteins is mediated by the recognition of phosphoserine. *Cell* **84,** 889–897
3. Yaffe, M. B., Rittinger, K., Volinia, S., Caron, P. R., Aitken, A., Leffers, H., Gamblin, S. J., Smerdon, S. J., and Cantley, L. C. (1997) The structural basis for 14-3-3: phosphopeptide binding specificity. *Cell* **91,** 961–971
4. Fuglsang, A. T., Borch, J., Bych, K., Jahn, T. P., Roepstorff, P., and Palmgren, M. G. (2003) The binding site for regulatory 14-3-3 protein in plant plasma membrane H^+-ATPase. Involvement of a region promoting phosphorylation-independent interaction in addition to the phosphorylation-dependent C-terminal end. *J. Biol. Chem.* **278,** 42266–42272
5. Chaudhri, M., Scarabel, M., and Aitken, A. (2003) Mammalian and yeast 14-3-3 isoforms form distinct patterns of dimmers *in vivo*. *Biochem. Biophys. Res. Commun.* **300,** 679–685
6. Pozuelo-Rubio, M., Geraghty, K. M., Wong, B. H. C., Wood, N. T., Campbell, D., Morrice, N., and MacKintosch, C. (2004) 14-3-3-affinity purification of over 200 human phosphoproteins reveals new links to regulation of cellular metabolism, proliferation and trafficking. *Biochem. J.* **379,** 395–408
7. Meek, S. E. M., Lane, W. S., and Piwnica-Worms, H. (2004) Comprehensive proteomic analysis of interphase and mitotic 14-3-3-binding proteins. *J. Biol. Chem.* **279,** 32046–32054
8. Jin, J., Smith, F. D., Stark, C., Wells, C. D., Fawcett, J. P., Kulkarni, S., Metalnikov, P., O'Donnell, P., Taylor, P., Taylor, L., Zougman, A., Woodgett, J. R., Langeberg, L. K., Scott, J. D., and Pawson, T. (2004) Proteomic, functional, and domain-based analysis of *in vivo* 14-3-3 binding proteins involved in cytoskeletal regulation and cellular organization. *Curr. Biol.* **14,** 1436–1450
9. Brajenovic, M., Joberty, G., Kuster, B., Bouwmeester, T., and Drewes, G. (2004) Comprehensive proteomic analysis of human Par protein complexes reveals an interconnected protein network. *J. Biol. Chem.* **279,** 12804–12811
10. Bauer, A., and Kuster, B. (2003) Affinity purification-mass spectrometry. Powerful tools for the characterization of protein complexes. *Eur. J. Biochem.* **270,** 570–578

11. Bouwmeester, T., Bauch, A., Ruffner, H., Angrand, P.-O., Bergamini, G., Croughton, K., Cruciat, C., Eberhard, D., Gagneur, J., Ghidelli, S., *et al.* (2004) A physical and functional map of the human TNF-α/NF-κB signal transduction pathway. *Nat. Cell Biol.* **6,** 97–105
12. Xing, H., Zhang, S., Weinheimer, C., Kovacs, A., and Muslin, A. J. (2000) 14-3-3 proteins block apoptosis and differentially regulate MAPK cascades. *EMBO J.* **19,** 349–358
13. Schorpp, M., Jäger, R., Schellander, K., Schenkel, J., Wagner, E. F., Weiher, H., and Angel, P. (1996) The human ubiquitin C promoter directs high ubiquitous expression of transgenes in mice. *Nucleic Acids Res.* **24,** 1787–1788
14. Nagy, A., Gertsenstein, M., Vintersten, K., and Behringer, R. (2002) *Manipulating the Mouse Embryo*, 3rd Ed., Cold Spring Harbor Laboratory Press, Cold Spring Harbor, NY
15. Rigaut, G., Shevchenko, A., Rutz, B., Wilm, M., Mann, M., and Seraphin, B. (1999) A generic protein purification method for protein complex characterization and proteome exploration. *Nat. Biotechnol.* **17,** 1030–1032
16. Shevchenko, A., Wilm, M., Vorm, O., and Mann, M. (1996) Mass spectrometric sequencing of proteins from silver-stained polyacrylamide gels. *Anal. Chem.* **68,** 850–858
17. Perkins, D. N., Pappin, D. J., Creasy, D. M., and Cottrell, J. S. (1999) Probability-based protein identification by searching sequence databases using mass spectrometry data. *Electrophoresis* **20,** 3551–3567
18. Fantl, W. J., Muslin, A. J., Kikuchi, A., Martin, J. A., MacNicol, A. M., Gross, R. W., and Williams, L. T. (1994) Activation of Raf-1 by 14-3-3 proteins. *Nature* **371,** 612–614
19. Conklin, D. S., Galaktionov, K., and Beach, D. (1995) 14-3-3 proteins associate with cdc25 phosphatases. *Proc. Natl. Acad. Sci. U. S. A.* **92,** 7892–7896
20. Craparo, A., O'Neill, T. J., and Gustafson, T. A. (1995) Non-SH2 domains within insulin receptor substrate-1 and SHC mediate their phosphotyrosine-dependent interaction with the motif of the insulin-like growth factor I receptor. *J. Biol. Chem.* **270,** 15639–15643
21. Grozinger, C. M., and Schreiber, S. L. (2000) Regulation of histone deacetylase 4 and 5 and transcriptional activity by 14-3-3-dependent cellular localization. *Proc. Natl. Acad. U. S. A.* **97,** 7835–7840
22. Zha, J., Harada, H., Yang, E., Jockel, J., and Korsmeyer, S. J. (1996) Serine phosphorylation of death agonist BAD in response to survival factor results in binding to 14-3-3 not BCL-X(L). *Cell* **87,** 619–628
23. van Rompay, A. R., Johansson, M., and Karlsson, A. (1999) Identification of a novel human adenylate kinase: cDNA cloning, expression analysis, chromosome localization and characterization of the recombinant protein. *Eur. J. Biochem.* **261,** 509–516
24. Matthews, J. M., and Visvader, J. E. (2003) LIM-domain-binding protein 1: a multifunctional cofactor that interacts with diverse proteins. *EMBO Rep.* **4,** 1132–1137
25. Loughney, K., Martins, T., Harris, E. A. S., Sadhu, K., Hicks, J. B., Sonnenburg, W. K., Beavo, J. A., and Ferguson, K. (1996) Isolation and characterization of cDNAs corresponding to two human calcium, calmodulin-regulated, 3′,5′-cyclic nucleotide phosphodiesterases. *J. Biol. Chem.* **271,** 796–806
26. Miyoshi, J., and Takai, Y. (2004) Dual role of DENN/MADD (Rab3GEP) in neurotransmission and neuroprotection. *Trends Mol. Med.* **10,** 476–480
27. Versteege, I., Sevenet, N., Lange, J., Rousseau-Merck, M.-F., Ambros, P., Handgretinger, R., Aurias, A., and Delattre, O. (1998) Truncating mutations of hSNF5/INI1 in aggressive paediatric cancer. *Nature* **394,** 203–206
28. Turelli, P., Doucas, V., Craig, E., Mangeat, B., Klages, N., Evans, R., Kalpana, G., and Trono, D. (2001) Cytoplasmic recruitment of INI1 and PML on incoming HIV preintegration complexes: interference with early steps of viral replication. *Mol. Cell* **7,** 1245–1254
29. Roberts, C. W. M., Galusha, S. A., McMenamin, M. E., Fletcher, C. D. M., and Orkin, S. H. (2000) Haploinsufficiency of Snf5 (integrase interactor 1) predisposes to malignant rhabdoid tumors in mice. *Proc. Natl. Acad. Sci. U. S. A.* **97,** 13796–13800
30. Vincenz, C., and Dixit, V. M. (1996) 14-3-3 proteins associate with A20 in an isoform-specific manner and function both as chaperone and adapter molecules. *J. Biol. Chem.* **271,** 20029–20034
31. Peng, C. Y., Graves, P. R., Ogg, S., Thoma, R. S., Byrnes, M. J., III, Wu, Z., Stephenson, M. T., and Piwnica-Worms, H. (1998) C-TAK1 protein kinase phosphorylates human Cdc25C on serine 216 and promotes 14-3-3 protein binding. *Cell Growth Differ.* **9,** 197–208
32. Shiraishi, Y., Mizutani, A., Yuasa, S., Mikoshiba, K., and Furuichi, T. (2004) Differential expression of Homer family proteins in the developing mouse brain. *J. Comp. Neurol.* **473,** 582–599
33. de Bartolomeis, A., and Iasevoli, F. (2003) The Homer family and the signal transduction system at glutamatergic postsynaptic density: potential role in behavior and pharmacotherapy. *Psychopharmacol. Bull.* **37,** (Summer) 51–83
34. Premont, R. T., Perry, S. J., Schmalzigaug, R., Roseman, J. T., Xing, Y., and Claing, A. (2004) The GIT/PIX complex: an oligomeric assembly of GIT family ARF GTPase-activating proteins and PIX family Rac1/Cdc42 guanine nucleotide exchange factors. *Cell. Signal.* **16,** 1001–1011
35. Zhang, H., Webb, D. J., Asmussen, H., and Horwitz, A. F. (2003) Synapse formation is regulated by the signaling adaptor GIT1. *J. Cell Biol.* **161,** 131–142
36. Gingras, A.-C., Aebersold, R., and Raught, B. (2005) Advances in protein complex analysis using mass spectrometry. *J. Physiol.* **563,** 11–21
37. Muller, J., Ory, S., Copeland, T., Piwnica-Worms, H., and Morrison, D. K. (2001) c-TAK1 regulates Ras signaling by phosphorylating the MAPK scaffold, KSR1. *Mol. Cell* **8,** 983–993
38. Sekimoto, T., Fukumoto, M., and Yoneda, Y. (2004) 14-3-3 suppresses the nuclear localization of threonine 157-phosphorylated $p27^{Kip1}$. *EMBO J.* **23,** 1934–1942
39. Uemura, T., Mori, H., and Mishina, M. (2004) Direct interaction of GluRδ2 with Shank scaffold proteins in cerebellar Purkinje cells. *Mol. Cell. Neurosci.* **26,** 330–341
40. Feng, Q., Baird, D., and Cerione, R. A. (2004) Novel regulatory mechanisms for the Dbl family guanine nucleotide exchange factor Cool-2/α-Pix. *EMBO J.* **23,** 3492–3504
41. Segal, M. (2005) Dendritic spines and long-term plasticity. *Nat. Rev. Neurosci.* **6,** 277–284